CORE
Metadata, citation and similar papers at core.ac
Provided by University of Queensland eSpace

MOLECULAR AND CELLULAR BIOLOGY, Jan. 2000, p. 416–427 Vol. 20, No. 1
0270-7306/00/$04.00+0
Copyright © 2000, American Society for Microbiology. All Rights Reserved.

Characterization of Insulin-Responsive GLUT4 Storage Vesicles Isolated from 3T3-L1 Adipocytes

MITSURU HASHIRAMOTO[1]† AND DAVID E. JAMES[1,2]*

Centre for Molecular and Cellular Biology[1] and Department of Physiology and Pharmacology,[2] University of Queensland, Brisbane, Queensland 4072, Australia

Received 18 August 1999/Accepted 20 September 1999

Insulin regulates glucose transport in muscle and adipose tissue by triggering the translocation of a facilitative glucose transporter, GLUT4, from an intracellular compartment to the cell surface. It has previously been suggested that GLUT4 is segregated between endosomes, the trans-Golgi network (TGN), and a postendosomal storage compartment. The aim of the present study was to isolate the GLUT4 storage compartment in order to determine the relationship of this compartment to other organelles, its components, and its presence in different cell types. A crude intracellular membrane fraction was prepared from 3T3-L1 adipocytes and subjected to iodixanol equilibrium sedimentation analysis. Two distinct GLUT4-containing vesicle peaks were resolved by this procedure. The lighter of the two peaks (peak 2) was comprised of two overlapping peaks: peak 2b contained recycling endosomal markers such as the transferrin receptor (TfR), cellubrevin, and Rab4, and peak 2a was enriched in TGN markers (syntaxin 6, the cation-dependent mannose 6-phosphate receptor, sortilin, and sialyltransferase). Peak 1 contained a significant proportion of GLUT4 with a smaller but significant amount of cellubrevin and relatively little TfR. In agreement with these data, internalized transferrin (Tf) accumulated in peak 2 but not peak 1. There was a quantitatively greater loss of GLUT4 from peak 1 than from peak 2 in response to insulin stimulation. These data, combined with the observation that GLUT4 became more sensitive to ablation with Tf-horseradish peroxidase following insulin treatment, suggest that the vesicles enriched in peak 1 are highly insulin responsive. Iodixanol gradient analysis of membranes isolated from other cell types indicated that a substantial proportion of GLUT4 was targeted to peak 1 in skeletal muscle, whereas in CHO cells most of the GLUT4 was targeted to peak 2. These results indicate that in insulin-sensitive cells GLUT4 is targeted to a subpopulation of vesicles that appear, based on their protein composition, to be a derivative of the endosome. We suggest that the biogenesis of this compartment may mediate withdrawal of GLUT4 from the recycling system and provide the basis for the marked insulin responsiveness of GLUT4 that is unique to muscle and adipocytes.

Glucose transport into mammalian cells is mediated by a facilitative carrier protein. Insulin regulates this transport process in muscle and adipose tissue by provoking the translocation of the glucose carrier GLUT4 from an intracellular storage compartment to the cell surface (5, 49). It is generally accepted that GLUT4 translocation is the major mechanism to account for increased glucose uptake in these tissues (1, 17). However, there is still debate concerning the nature of the intracellular GLUT4 compartment in insulin-sensitive cells.

A major characteristic of GLUT4 is that in the basal state it is excluded from the cell surface due to its sequestration in intracellular tubules and vesicles (42). Insulin causes a 10- to 40-fold increase in the plasma membrane (PM) levels of GLUT4, whereas most other proteins, such as the transferrin receptor (TfR) and the mannose 6-phosphate receptor (MPR), increase only by a factor of 2 to 3 (51, 52). An additional protein referred to as vp165 or gp160, also known as insulin-responsive aminopeptidase (IRAP), which is targeted similarly to GLUT4 in adipocytes, has been described, and this protein also undergoes a 10- to 40-fold increase in response to insulin stimulation (19, 37). This differential effect of insulin on GLUT4 versus other recycling proteins is presumably a function of a unique intracellular trafficking step resulting in the withdrawal of GLUT4 from the normal recycling pathway into a compartment that can readily exchange with the cell surface in response to stimuli such as insulin.

By immunoelectron microscopy, GLUT4 has been localized to several elements of the recycling pathway, including the trans-Golgi network (TGN), clathrin-coated vesicles, and endosomes. However, in insulin-sensitive cells the vast majority of GLUT4 is found in tubulovesicular elements clustered in the cytoplasm (42, 43). Although at present it is not clear if these tubulovesicular elements are subdomains of the endosomal-TGN system or a discrete specialized secretory system like small synaptic vesicles in neurons, there are several indications that GLUT4 may be sequestered in a specialized compartment in fat and muscle cells. First, double-label immunofluorescence microscopy of insulin-sensitive cells has revealed differential intracellular targeting of GLUT4 and GLUT1 (34). Second, GLUT4 is enriched in regulated secretory granules when expressed in endocrine cells, indicating the presence of specialized sorting signals in this protein (13, 44). Third, the discovery of IRAP, a protein that behaves similarly to GLUT4 in adipocytes, is consistent with the biogenesis of a compartment that may undergo exocytosis in response to insulin stimulation (18, 19, 21, 28). In spite of these observations, it has been difficult to isolate vesicles that have the characteristics of such a compartment from insulin-sensitive cells, which makes it difficult to distinguish between the different models that have been postulated.

In the present study, we have utilized several approaches,

* Corresponding author. Mailing address: Centre for Molecular & Cellular Biology, University of Queensland, Brisbane, Queensland 4072, Australia. Phone: 61-7-33654986. Fax: 61-7-33654388. E-mail: D.James@cmcb.uq.edu.au.

† Present address: Second Department of Internal Medicine, Kobe University School of Medicine, Chuo-Ku, Kobe 650-0017, Japan.

Downloaded from http://mcb.asm.org/ on October 26, 2015 by University of Queensland Library

including vesicle immunoadsorption and iodixanol equilibrium sedimentation analysis in combination with the transferrin (Tf)-horseradish peroxidase (HRP)–3,3′-diaminobenzidine (DAB)-mediated endosomal ablation technique to isolate and characterize different populations of GLUT4-containing vesicles in 3T3-L1 adipocytes. We have identified a population of vesicles that are distinct from both recycling endosomes and TGN and that are highly insulin responsive. These data provide evidence for the existence of a unique exocytic storage compartment that is abundant in insulin-sensitive cells and that may be a derivative of the endosomal-TGN system.

MATERIALS AND METHODS

Materials. Male Wister rats were obtained from the Animal Resources Centre (Perth, Western Australia, Australia), and ^{125}I-Tf was obtained from NEN (Boston, Mass.). Human apo Tf, holo Tf, type VI HRP, and DAB were obtained from Sigma (St. Louis, Mo.). Protein G-Sepharose and polyvinylidene difluoride blotting membranes were obtained from Amersham Pharmacia Biotech Inc. (Uppsala, Sweden). Bovine serum albumin (BSA) was obtained from ICN Biomedical Inc. (Aurora, Ohio), Iodixanol (Optiprep) was purchased from Life Technologies, Inc. (Milan, Italy).

The following antibodies were used in these studies: 1F8, a monoclonal antibody specific for GLUT4 (14); R820, a rabbit polyclonal antibody raised against a synthetic peptide corresponding to the COOH-terminal 12 amino acids of rat GLUT4 (16) and used for immunoblotting; R017, a rabbit polyclonal antibody raised against a synthetic peptide corresponding to the COOH-terminal 20 amino acids of rat GLUT4 and used for immunofluorescence microscopy; a rabbit polyclonal antibody against the N terminus of IRAP (21); a rabbit polyclonal antibody raised against a C-terminal synthetic peptide from rat sortilin (CKSGYHDDSDEDLLE) (31) (provided by G. Lienhard, Dartmouth University, Hanover, N.H.); a rabbit polyclonal antibody against the cytoplasmic domain of human cation-dependent MPR (CD-MPR) (provided by A. Hille-Rehfeld, University of Göttingen, Göttingen, Germany); a mouse monoclonal antibody against the cytoplasmic tail of the TfR (Zymed, San Francisco, Calif.); a polyclonal antibody against syntaxin 6 (2); a rabbit polyclonal antibody against the N terminus of vesicle-associated membrane protein 2 (VAMP2) (32) (provided by M. Takahashi, Mitsubishi Kasei Institute of Life Science, Machida, Japan); a rabbit polyclonal antibody against the N terminus of cellubrevin (53); a rabbit polyclonal antibody against Rab4 (55) (provided by Peter van der Sluijs, University of Utrecht, Utrecht, The Netherlands), a rabbit polyclonal antibody against Rab11 (54) (provided by R. G. Parton, University of Queensland, Brisbane, Australia); a polyclonal vesicular stomatitis virus glycoprotein (VSV-G) antibody (provided by T. Nilsson, European Molecular Biology Laboratory, Heidelberg, Germany); and a mouse monoclonal antibody against VSV-G (P5D4; Boehringer Mannheim).

Cell culture and subcellular fractionation. Murine 3T3-L1 fibroblasts were cultured in Dulbecco's modified Eagle's medium (DMEM) (GIBCO BRL, Gaithersburg, Md.) supplemented with newborn calf serum, 2 mM L-glutamate, 100 U of penicillin per liter, and 100 mg of streptomycin per liter at 37°C in an atmosphere of 5% CO_2. Confluent cells were differentiated into adipocytes as described previously (8), grown in DMEM supplemented with 10% fetal calf serum (FCS), and used at 8 to 12 days after differentiation. 3T3-L1 adipocytes were incubated in serum-free DMEM for 16 h to establish a basal condition and stimulated with 10^{-7} M insulin for 20 min at 37°C as indicated below. The cells were rinsed three times with HES buffer (20 mM HEPES–1 mM EDTA–250 mM sucrose [pH 7.4]) on ice and scraped with a rubber policeman in HES buffer containing 250 μM phenylmethylsulfonyl fluoride, 10 μg of aprotinin per ml, and 10 μg of leupeptin per ml. Subcellular fractionation was carried out as described previously (40) to obtain PM, high density microsome, and low density microsome (LDM) fractions. Chinese hamster ovary (CHO) cells expressing the wild-type GLUT4 (35) were cultured in DMEM supplemented with 10% FCS, 2 mM L-glutamate, 100 U of penicillin per ml, and 100 mg of streptomycin per ml at 37°C in an atmosphere of 5% CO_2. Confluent cells were scraped and homogenized by being passed 10 times through a 22-gauge needle. The homogenate was centrifuged in a Sorvall SS-34 rotor (DuPont Co., Newton, Conn.) at 27,000 × g_{max} (where g_{max} is the maximum force of gravity) for 15 min, and the resultant supernatant was centrifuged in a Ti80 rotor (Beckman) at 235,000 × g_{max} for 75 min to obtain the LDM fraction.

Expression of sialyltransferase. CHO cells were transiently transfected with pSRα-VSV-G-tagged human sialyltransferase cDNA (a gift from T. Nilsson, European Molecular Biology Laboratory) (36) by using LipofectAMINE reagent (Life Technologies, Gaithersburg, Md.) according to the manufacturer's instructions. In brief, subconfluent cells were washed with Opti-mem reduced serum (Life Technologies) and incubated in the presence of a concentration of DNA and LipofectAMINE (2 μg of DNA/10 μl of LipofectAMINE) for 5 to 7 h. The medium was replaced with DMEM supplemented with 10% FCS without antibiotics and incubated overnight. Cells were processed for immunofluorescence or subcellular fractionation at 48 h posttransfection. VSV-G-tagged human sialyltransferase cDNA was subcloned as a *Bam*HI fragment from pSRα into the retroviral expression vector, pBABEpuro (29). Retroviral stocks of pBABE-sialyltransferase were generated with the BOSC23 packaging cell line (33). In brief, heterogeneous pools of 3T3-L1 adipocytes stably expressing the construct were produced by infecting subconfluent (50 to 70%) 3T3-L1 fibroblasts for 5 to 7 h with virus in the presence of 4 μg of Polybrene per ml. After 48 h of infection, the cells were treated with trypsin and plated at 1:5 in DMEM supplemented with 10% FCS in the presence of 2 μg of puromycin (Sigma) per ml. Puromycin-resistant cells were allowed to grow to confluence and were then differentiated as described above.

Isolation of rat adipocytes and skeletal muscle. Primary adipocytes were prepared from epididymal fat pads of male 150- to 200-g Wister rats by the collagenase digestion method (40). To establish basal conditions, isolated rat adipocytes were incubated for 30 min in Krebs-Ringer phosphate (KRP) buffer (12.5 mM HEPES, 120 mM NaCl, 6 mM KCl, 1.2 mM $MgSO_4$, 1 mM $CaCl_2$, 1 mM sodium phosphate) containing 2.5 mM D-glucose and 2% BSA, pH 7.4. Rat skeletal muscle (tibialis muscle) was dissected out, minced in HES buffer, and homogenized with a Polytron (Lucerne, Switzerland) model PCU-2 and then further homogenized by 10 passes through a tight-fitting Potter-Elvehjem homogenizer at 800 rpm. The homogenate was centrifuged for 15 min at 3,000 × g at 4°C, and the supernatant was centrifuged again for 15 min at 10,000 × g at 4°C. The resultant supernatant was layered onto a discontinuous sucrose gradient containing layers of 0.4 and 1.5 M sucrose prepared in 20 mM HEPES–1 mM EDTA (pH 7.4) and centrifuged in an SW41 rotor (Beckman) at 200,000 × g_{av} (where g_{av} is the average force of gravity) for 90 min at 4°C. The LDM fraction at the 0.4-1.5 M sucrose interface was removed and used for iodixanol equilibrium gradient centrifugation.

Vesicle immunoadsorption. The LDM fraction of isolated adipocytes or 3T3-L1 adipocytes was resuspended in phosphate-buffered saline (PBS) and layered onto a continuous sucrose gradient (5 to 32%) made up in 20 mM HEPES–1 mM EDTA (pH 7.4) and centrifuged in a Beckman SW41 rotor at 91,000 × g_{av} for 2.5 h. Fractions collected from the top of the gradient were analyzed by immunoblotting for GLUT4. A single peak of GLUT4 was obtained in the middle of the gradient. These fractions were pooled and used for vesicle immunoadsorption. The LDM fraction from 3T3-L1 adipocytes was sedimented by iodixanol equilibrium gradient as described below, and the separate fractions (fractions 2 to 4 for peak 1 and fractions 9 to 11 for peak 2) were pooled and used for vesicle immunoadsorption.

Monoclonal antibodies (1F8 and the irrelevant antibody) were partially purified by ammonium sulfate precipitation followed by Q Sepharose anion-exchange chromatography. In the experiment to immunoadsorb GLUT4 vesicles from rat adipocytes, purified antibodies were coupled to protein G-Sepharose beads (Pharmacia) at a concentration of 10 μg of immunoglobulin G/10 μl of resin for 16 h at 4°C in PBS containing 0.5% BSA by end-over-end rotation. In the experiment to immunoadsorb GLUT4 vesicles from 3T3-L1 adipocytes, purified antibodies were conjugated to activated cellulose fibers as described previously (10), with slight modifications. Briefly, purified antibody was directly coupled to the cellulose at 1 mg of immunoglobulin G/mg of cellulose in 200 mM borate buffer (pH 8.2) for 24 h by end-over-end rotation. Fibers were subsequently incubated with 100 mM glycine–100 mM borate buffer (pH 8.2) and then 100 mM borate buffer containing 1% BSA. Beads and fibers were washed three times with PBS, and the antibodies were cross-linked to the resin by incubation for 30 min at room temperature in a solution containing 20 mM dimethyl suberimidate (Pierce, Rockford, Ill.), 50 mM borate, and 3 M NaCl (pH 9.0). The beads and fibers were then blocked with 0.2 M ethanolamine (pH 8.0; Sigma), washed three times with PBS, and stored at 4°C until use. Vesicle immunoadsorption was carried out by incubating 100 μl of antibody-coupled protein G beads with the pooled sucrose gradient fractions derived from 1 mg of original LDM or 100 μg of antibody-coupled cellulose fibers with the pooled iodixanol fractions (peak 1 or peak 2) derived from 1 mg of original LDM for 2 h at 4°C on a rotating wheel in 1 ml of PBS (pH 7.4) containing 1% BSA. Control immunoadsorptions were performed in which incubations were carried out with either beads and fibers alone or beads and fibers coupled with an irrelevant monoclonal antibody. After the incubation, beads and fibers were washed three times with PBS and the immunoadsorbed vesicles were eluted off the beads and fibers by incubation with 0.2 M bicarbonate buffer (pH 11.0) for 30 min on ice. Eluted vesicles were finally pelleted at 210,000 × g_{max} in a Beckman TLA100.3 rotor and analyzed by sodium dodecyl sulfate-polyacrylamide gel electrophoresis (SDS-PAGE) and silver staining.

Microsequencing. Bicarbonate-eluted sample from a large-scale vesicle preparation (25 mg of rat adipocyte LDM) was electrophoresed in a single large slab gel lane. Polypeptides were transferred electrophoretically in 10 mM 3-[cyclohexylamino]-1-propanesulfonic acid (CAPS) (Sigma)–10% methanol buffer (pH 11.0) to ProBlott membrane (Applied Biosystems, Foster City, Calif.) and stained with Coomassie brilliant blue. Protein bands that were highly enriched in the 1F8 immunoprecipitate were excised and subjected to N-terminal sequencing at the Protein Chemistry Facility, LaTrobe University, Melbourne, Australia.

Iodixanol equilibrium gradient centrifugation. The LDM fraction prepared from 3T3-L1 adipocytes as described above was resuspended in HES buffer. The LDM was mixed with iodixanol (Optiprep) to a 14.0% final concentration, and the resultant sucrose concentration in the mixture was 190 mM. A self-generating gradient was formed in a 4.0-ml sealed tube (Nalge, Rochester, N.Y.) by centri-

Downloaded from http://mcb.asm.org/ on October 26, 2015 by University of Queensland Library

fuging to equilibrium at 4°C with a VTi65.2 vertical rotor (Beckman) at 265,000 × g_{av} for 4 h. In experiments analyzing the LDM obtained from cells incubated with Tf-HRP, the gradients were sedimented at 265,000 × g_{av} for 5 h. Fractions (~0.3 ml) were collected from the bottom of the tube and analyzed by immunoblotting.

Preparation of the Tf-HRP conjugate, Tf-HRP endosomal ablation, and DAB cytochemistry. The Tf-HRP conjugate (Tf-HRP) was prepared as described previously (46) with slight modifications. In brief, human apo Tf was coupled, in the presence of ~10^7 cpm of ^{125}I-labelled human diferric Tf as a tracer, to type VI HRP with *N*-succinimidyl-3-[2-pyridylthio]propionate (SPDP) (Pharmacia) as the coupling agent according to the manufacturer's instructions. The Tf-HRP conjugate was separated from free HRP and Tf on a Sephacryl S-200 HR 16/60 column (Pharmacia) in 20 mM Tris HCl–150 mM NaCl (pH 7.2) by a Pharmacia fast-performance liquid chromatography system. Fractions were analyzed by SDS-PAGE, and those containing monomeric Tf-HRP conjugate were pooled, concentrated with a Centricon concentrator (Amicon, Beverly, Mass.), and again passed over a Sephacryl S-200 HR 16/60 column in the same buffer to achieve higher purification. Fractions from the second gel filtration were again pooled, analyzed by SDS-PAGE and autoradiography, concentrated, and iron loaded by dialyzing for 4 h against 10 mM $NaHCO_3$–2 mM sodium nitrilotriacetate–0.25 mM $FeCl_3$–250 mM Tris HCl (ph 8.0). The final product was dialyzed four times against 20 mM HEPES–NaOH (pH 8.2)–150 mM NaCl to remove excess iron. The concentration of the Tf-HRP conjugate was measured with a protein assay reagent (Bio-Rad, Hercules, Calif.) with Tf as a standard. The conjugate was then aliquoted and stored at −70°C until use.

DAB cytochemistry was performed with 3T3-L1 adipocytes as described previously (25), with some modifications. Cells were starved in DMEM–20 mM HEPES–NaOH (pH 7.2) (DME-H) for 16 h and incubated at 37°C in DME-H containing 25 μg of Tf-HRP conjugate per ml for 60 min. As indicated below, cells were stimulated with 10^{-7} M insulin for 20 min prior to the addition of the conjugate, and insulin was kept in DME-H throughout the incubation with Tf-HRP. Cells were chilled on ice and washed once with ice-cold DME-H and then with three changes of ice-cold citrate buffer (20 mM sodium citrate–150 mM NaCl [pH 5.0]) to remove surface-bound Tf-HRP. The cell monolayer was finally washed once in ice-cold PBS (pH 7.4) before DAB cytochemistry. DAB was freshly prepared as a 2-mg/ml stock, filtered through a 0.22-μm-pore-size filter, and added to cells at the concentrations indicated below in 20 mM HEPES–70 mM NaCl (pH 7.0). H_2O_2 was added at a final concentration of 0.02% (vol/vol). After a 60-min incubation at 4°C in the dark, the reaction was quenched by washing with ice-cold PBS containing 0.5% BSA and three subsequent washes in ice-cold HES buffer. The cells were then scraped in HES buffer and fractionated as described above. In all experiments, duplicate plates, one of which was exposed to DAB and H_2O_2 and the other of which was exposed only to DAB as a control, were prepared.

TfR internalization. 3T3-L1 adipocytes in 10-cm culture plates were serum starved in DMEM for 16 h, washed three times with warm KRP buffer at 37°C, and incubated at 37°C for 2 min in warm KRP buffer containing ~3.0 μCi of ^{125}I-labelled diferric human Tf (NEN) per 10-cm plate and 1 mg of BSA per ml. Nonspecific uptake was measured in a duplicate plate by including excess (20 μM) unlabelled holo Tf. After two quick washes with warm KRP buffer, the cells were further incubated at 37°C for the times indicated below to allow TfR internalization. Uptake was terminated by two washes on ice with KRP and a further 8-min wash with ice-cold acid wash buffer (20 mM sodium citrate–150 mM NaCl [pH 5.0]) to remove surface-bound Tf. The cells were finally washed three times with HES buffer, scraped, and subjected to the subcellular fractionation procedure as described above.

Indirect immunofluorescence. CHO cells stably expressing GLUT4 (35) or the human TfR (kindly provided by Tim McGraw, Cornell University, New York, N.Y.) were transiently transfected with VSV-G-tagged sialyltransferase cDNA as described above. In the case of TfR-expressing cells, Tf-conjugated Texas red was bound to the surface and internalized for 15 or 60 min. Cells were fixed with 2% paraformaldehyde and labelled with antibodies specific for the C terminus of GLUT4 and/or the VSV-G epitope (P5D4) in PBS containing 1% normal swine serum (Dako, Carpinteria, Calif.). Coverslips were washed with 0.1% BSA and incubated for 30 min with either fluorescein isothiocyanate (FITC)-conjugated anti-rabbit antibody alone or with FITC-conjugated anti-rabbit antibody plus a Texas red X-conjugated anti-mouse antibody (Molecular Probes, Eugene, Oreg.). Coverslips were washed with PBS, mounted, and viewed with a 63×, 1.4-numerical-aperture Zeiss oil immersion objective on a Zeiss Axiovert fluorescence microscope equipped with a Bio-Rad MRC-600 laser confocal imaging system. Unmodified images were printed by using Adobe Photoshop (Adobe Systems, Mountain View, Calif.).

SDS-PAGE and immunoblotting. SDS-PAGE was performed as described previously (23). Proteins resolved by SDS-PAGE were electrophoretically transferred to polyvinylidene difluoride membrane, immunoblotted with various antibodies as indicated above, and visualized by either the ECL detection system (Amersham, Aylesbury, United Kingdom) or the Immunostar enhanced chemiluminescence detection system (Bio-Rad), with either HRP-conjugated or alkaline phosphatase-conjugated secondary antibodies.

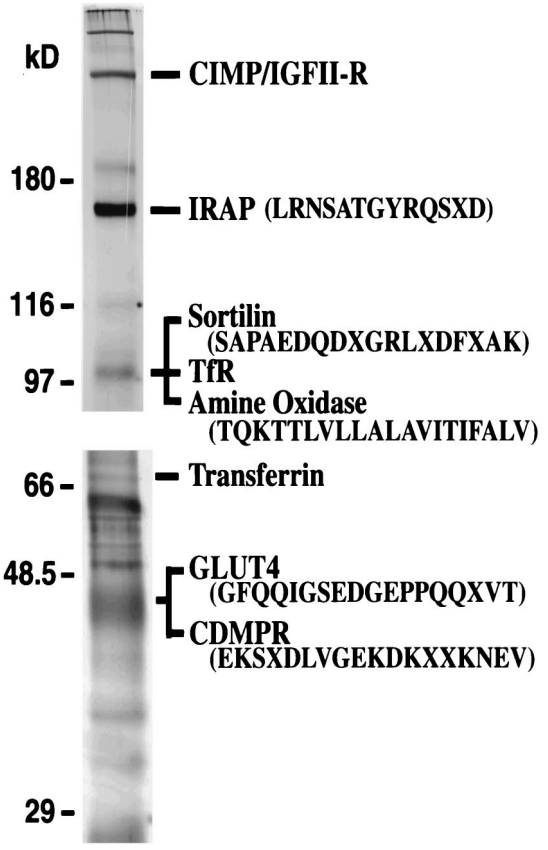

FIG. 1. Polypeptide composition of GLUT4-containing vesicles. Vesicle immunoadsorption was carried out by incubating protein G-Sepharose beads coupled to a purified monoclonal GLUT4 antibody (1F8) with pooled velocity sucrose gradient fractions isolated from rat adipocytes for 2 h at 4°C on a rotating wheel in PBS containing 0.1% BSA. After the incubation, beads were washed and the vesicles were eluted from the beads with 0.2 M bicarbonate buffer (pH 11.0). Eluted proteins were pelleted and analyzed by SDS-PAGE followed by silver staining. Proteins with molecular masses of 165, 110, and ~50 kDa from a large-scale vesicle preparation were excised and subjected to N-terminal sequencing. The amino acid sequences and identities of these proteins are shown at the right. Other proteins were identified by immunoblotting. The upper half is from a 6% resolving gel, and the bottom half is from a 10% gel. CIMP/IGFII-R, CI-MPR and insulin-like growth factor receptor II.

RESULTS

Polypeptide composition of GLUT4-containing vesicles. In order to approach the nature of the intracellular GLUT4 compartment, we initiated the study by characterizing the polypeptide composition of the GLUT4-containing vesicles. To accomplish this we used vesicle immunoadsorption, a technique that has previously been used by several groups to study GLUT4-containing vesicles (6, 10, 18, 19, 21, 22, 24, 28, 30, 31, 41). In Fig. 1 we show a silver stain depicting the major polypeptides in GLUT4-containing vesicles immunopurified from rat adipocytes. In order to generate this image we made several modifications to previous methods which optimized nonspecific binding. Firstly, the LDM fraction was subjected to velocity sucrose gradient analysis to further purify the intracellular GLUT4-containing vesicles prior to immunoadsorption. Secondly, the antibodies were cross-linked to the beads, thus avoiding the presence of antibody contaminants in the eluate. Finally, the immunopurified vesicles were eluted from the beads by using bicarbonate buffer. These strategies afforded a considerable reduction in nonspecific binding. In fact, none of

Downloaded from http://mcb.asm.org/ on October 26, 2015 by University of Queensland Library

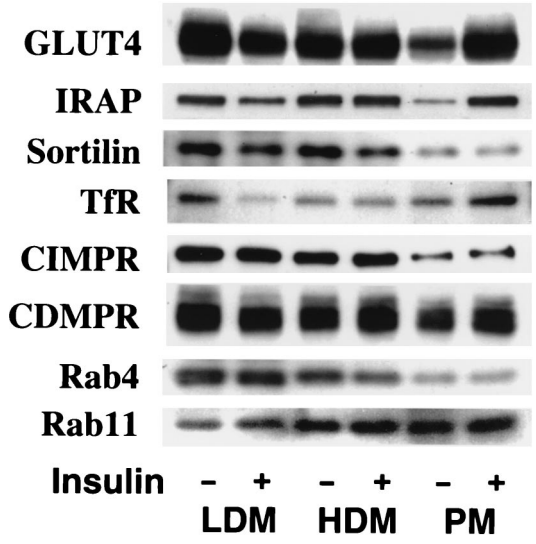

FIG. 2. The effect of insulin on the subcellular distributions of various proteins in 3T3-L1 adipocytes. 3T3-L1 adipocytes were incubated in the absence (−) or presence (+) of 10^{-7} M insulin for 20 min at 37°C. Subcellular fractionation was carried out to obtain plasma PM, high density microsome (HDM) and LDM fractions. Immunoblotting was carried out with specific antibodies as indicated. The results shown are from a single preparation of the membrane fractions and are representative of similar determinations.

the bands indicated in Fig. 1 were present in immunoadsorptions performed with control antibodies (data not shown).

The major proteins in the GLUT4-containing vesicles isolated by this approach were as follows: a 210-kDa band, identified as the insulin-like growth factor receptor II- and cation-independent MPR (CI-MPR), and an 80-kDa band, previously identified as Tf (10). Researchers in our laboratory have also identified the TfR in this compartment by using specific antibodies (10). Bands with relative molecular masses of 165 kDa, 100 kDa, and 45 kDa were excised from the gel and subjected to N-terminal amino acid sequencing. The 165-kDa band yielded one single sequence that corresponded to residues 88 to 100 (LRNSATGYRQSXD) of IRAP, in agreement with previous studies (18, 19, 21, 28). The 100-kDa band yielded two overlapping sequences corresponding to residues 2 to 21 (TQKTTLVLLALAVITIFALV) and 45 to 62 (SAPAEDQD XGRLXDFXAK) of rat amine oxidase (30) and sortilin (24, 31), respectively. Both of these proteins have been identified as constituents of GLUT4-containing vesicles by other groups (24, 30, 31). The 45-kDa band yielded two overlapping sequences corresponding to residues 4 to 21 (GFQQIGSE DGEPPQQXVT) and 40 to 57 (EKSXDLVGEKDKXXK NEV) of GLUT4 and the CD-MPR (50), respectively.

Effect of insulin on the subcellular distribution of polypeptides in 3T3-L1 adipocytes. To further characterize proteins that colocalize with GLUT4, we undertook a comprehensive study of the subcellular distribution of a number of different proteins in adipocytes treated with or without insulin. As shown in Fig. 2, many of the proteins that were found to be highly enriched in GLUT4-containing vesicles (Fig. 1), such as sortilin, TfR, CI-MPR, and CD-MPR, showed either a small (~2- to 3-fold) degree of insulin-dependent movement to the cell surface or no significant movement at all. Quantitation of the immunoblotting for these proteins in three different preparations revealed that the fold increases in the PM fractions upon insulin stimulation were 2.5 ± 1.1 (mean ± standard deviation [SD], $n = 3$) for the TfR and 3.5 ± 1.2 (mean ± SD, $n = 3$) for the CI-MPR, results that were essentially consistent with the results reported previously (51, 52). In contrast, insulin caused a large (>5-fold) insulin-dependent increase in cell surface levels of GLUT4 and IRAP. In addition, we observed

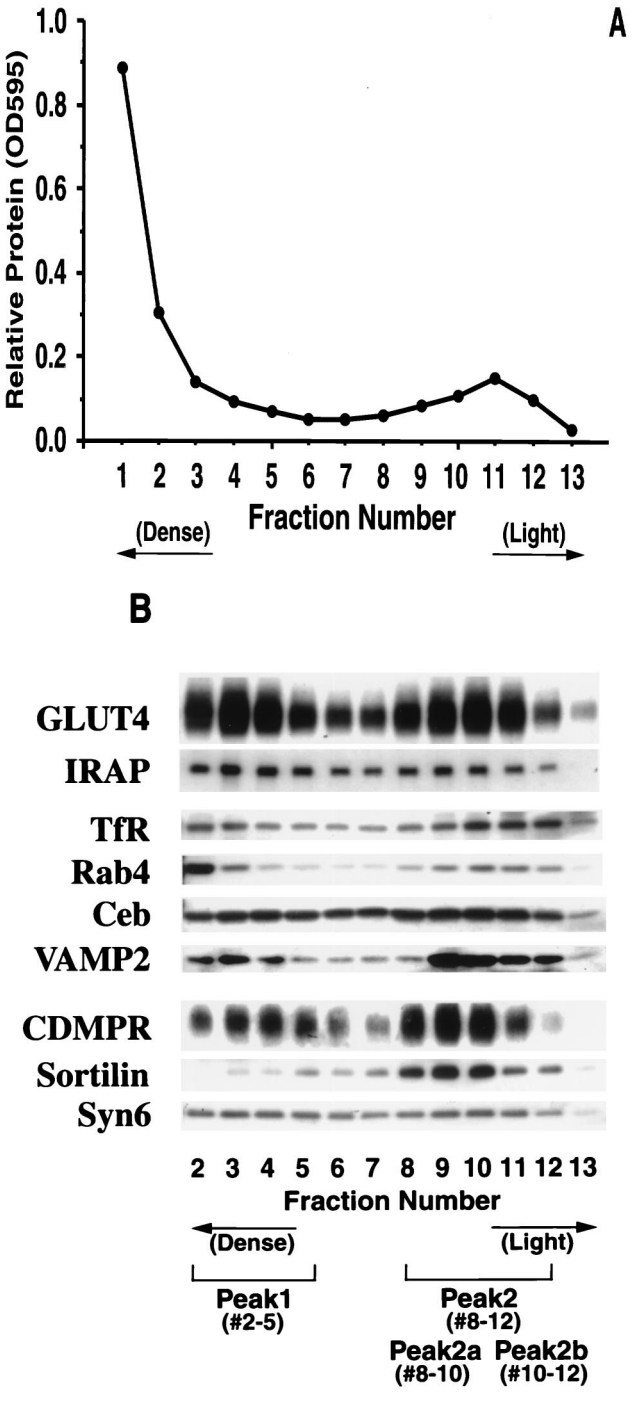

FIG. 3. Iodixanol equilibrium gradient sedimentation analysis of 3T3-L1 adipocytes. The LDM fraction prepared from 3T3-L1 adipocytes was subjected to iodixanol density gradient analysis as described in Materials and Methods. Fractions were collected from the bottom of the gradient and used to measure protein (A) or the distribution of various proteins by immunoblotting (B). Note that in panel B, fraction 1 is omitted from the immunoblotting analysis (see Results). The results shown are from a single iodixanol gradient analysis and are representative of six experiments. Syn6, syntaxin 6; Ceb, cellubrevin; OD595, optical density at 595 nm.

Downloaded from http://mcb.asm.org/ on October 26, 2015 by University of Queensland Library

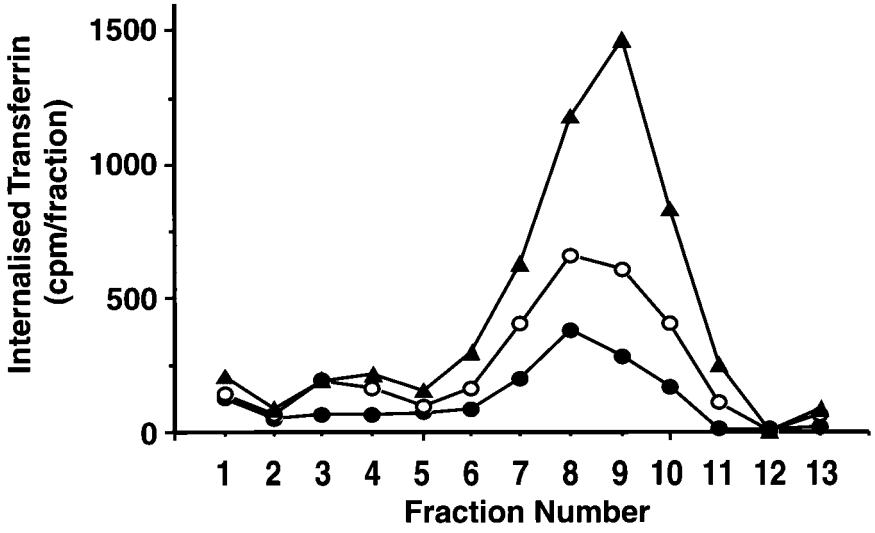

FIG. 4. Iodixanol equilibrium gradient sedimentation analysis of internalized Tf. 3T3-L1 adipocytes were serum starved in DMEM for 16 h and then incubated at 37°C for 2 min with KRP buffer containing ^{125}I-diferric human Tf (~1.0 μCi/ml) and BSA (1 mg/ml). As a control to estimate nonspecific uptake, duplicate plates were incubated in the presence of excess (20 μM) unlabelled holo Tf. After two quick washes, the cells were incubated at 37°C for 0 (●), 3 (○), and 20 (▲) min to allow Tf internalization. Cells were washed and subjected to subcellular fractionation and iodixanol sedimentation analysis as described in Materials and Methods. Fractions were counted in a gamma counter, and internalized Tf was quantitated by subtracting background values from each fraction. The results shown are representative of two separate experiments.

no effect of insulin on the subcellular distribution of Rab4 or Rab11 in 3T3-L1 adipocytes (54, 55).

Iodixanol equilibrium sedimentation analysis of 3T3-L1 adipocyte LDM. One interpretation of the above data is that GLUT4 is targeted to the endosomal-TGN system and that insulin selectively modulates the trafficking of this protein compared to that of others that are targeted to the same organelles. Another interpretation is that GLUT4 is selectively targeted to an intracellular storage compartment, possibly connected to the endosomal-TGN system and that techniques such as immunoadsorption may be inadequate for resolving such a compartment from the constitutive recycling pathway. This may be expected because it is clear that at least a portion of GLUT4 is targeted to endosomes and the TGN (42), and the immunoadsorption technique would not discriminate between vesicles derived from these origins and the storage compartment. It has also not been possible to resolve distinct intracellular GLUT4 compartments by using sucrose density gradients (15). However, if these different classes of vesicles are derived from a similar point of origin they may have similar characteristics, such as density and size, thus limiting this approach. Furthermore, the density of GLUT4-containing vesicles (~1.13 g/cm^3) coincides with a hyperosmotic concentration of sucrose (20) and this may also limit its resolving capacity. Recently a series of iodinated sedimentation media were developed to avoid this problem. In the present study we employed one of these media, iodixanol, in an equilibrium centrifugation analysis to segregate the crude intracellular GLUT4 vesicle fraction obtained from 3T3-L1 adipocytes (referred to as LDM) into two distinct peaks (Fig. 3B). We designated the denser peak (fractions 2 to 5) as peak 1, and the lighter peak (fractions 8 to 12) as peak 2. The distribution of GLUT4 between these two peaks was 44.3% ± 1.8% (mean ± standard error; $n = 8$) in peak 1 and 39.2% ± 2.5% (mean ± standard error; $n = 8$) in peak 2.

The majority of protein (~90%) in the starting fraction sedimented through the gradient into fraction 1 (Fig. 3A). This is consistent with the results of our previous studies (3, 12), showing that a large proportion of protein in this fraction comprises cytoskeletal or macromolecular protein complexes. In addition, it is conceivable that large membrane aggregates sediment to this position of the gradient. We routinely excluded fraction 1 from our analysis due to its very high protein content. The only other peak of protein routinely detected in the gradient coincided with peak 2.

Immunoblotting with antibodies specific for a variety of membrane protein markers revealed that peak 2 was comprised of two overlapping peaks. The lighter of these (peak 2b) was enriched in the TfR, Rab4 (Fig. 3B), and Rab11 (data not shown) and presumably corresponded to recycling endosomes. Peak 2a was highly enriched in sortilin. In addition, the CD-MPR and syntaxin 6 were enriched in this peak. The majority of GLUT4 and IRAP found in peak 2 coincided with peak 2a. Cellubrevin was more broadly distributed over both peak 2a and peak 2b. VAMP2 was enriched in fractions 9 to 12, a result which was characteristic of neither peak 2b nor peak 2a. Thus, it is conceivable that this represents an alternate intracellular compartment.

With the possible exception of sortilin, most of the proteins that were enriched in peak 2 were also found in peak 1. However, GLUT4 was more enriched in peak 1 than any other protein analyzed. Furthermore, the distribution of the TfR and Rab4 did not overlap exactly with GLUT4 in peak 1, suggesting that, like peak 2, peak 1 may be comprised of at least two separate vesicle populations. VAMP2, cellubrevin, IRAP, syntaxin6 and CD-MPR overlapped with GLUT4 in peak 1 suggesting that these proteins may colocalize in the same population of vesicles, consistent with previous immunoelectron microscopic experiments (26, 27). We reproducibly find that whereas membrane proteins such as GLUT4 and the CD-MPR are resolved into two distinct peaks by iodixanol density gradient analysis, other proteins, such as IRAP, syntaxin 6, and cellubrevin, although distributed between peak 1 and peak 2, are not as well resolved. This may reflect the extremely shallow depth of this gradient. Thus, this presumably represents the broader distribution of certain proteins among different vesicles. These data are also consistent with our previous observa-

Downloaded from http://mcb.asm.org/ on October 26, 2015 by University of Queensland Library

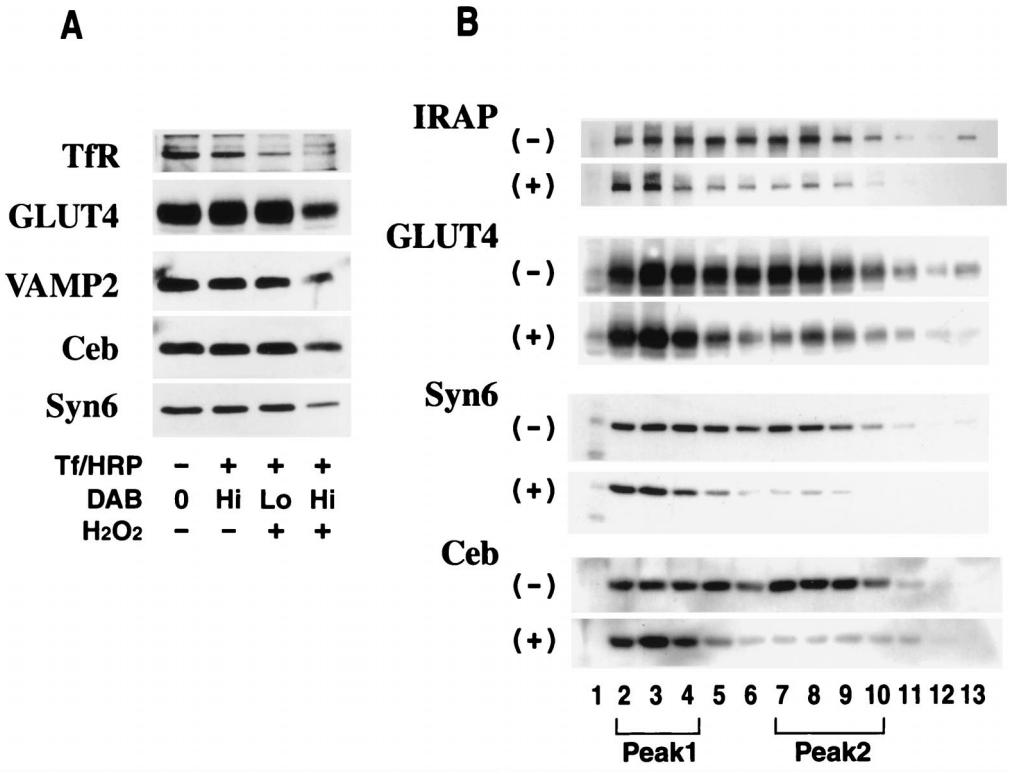

FIG. 5. Tf-HRP endosomal ablation in 3T3-L1 adipocytes. 3T3-L1 adipocytes were starved in DMEM for 16 h and incubated at 37°C for 60 min in DME-H containing 25 μg of Tf-HRP conjugate per ml. As indicated above, cells were stimulated with 10^{-7} M insulin for 20 min prior to the addition of the conjugate and insulin was kept in DME-H throughout the incubation with Tf-HRP. Cells were then chilled on ice and washed in low-pH buffer, and DAB was added at final concentrations of 50 μg/ml (Lo) and 250 μg/ml (Hi) for the blot shown in panel A and 250 μg/ml for the blot shown in panel B, in 20 mM HEPES–70 mM NaCl (pH 7.0). Cells were then incubated in the presence (+) or absence (−) of H_2O_2 (0.02%, vol/vol). After a 60-min incubation at 4°C in the dark, the reaction was quenched by washing with ice-cold PBS containing 0.5% BSA and three subsequent washes in ice-cold HES buffer. The cells were then subjected to subcellular fractionation to obtain the LDM fraction as described. The LDM was either immunoblotted directly (A) or subjected to iodixanol density gradient analysis before immunoblotting (B). For the blot shown in panel B, the iodixanol gradients were centrifuged for 5 h at 265,000 × g_{av}. The results shown are representative of three separate experiments. Syn6, syntaxin 6; Ceb, cellubrevin.

tions that IRAP and GLUT4 do not co-localize identically in insulin-sensitive cells (27).

Distribution of endocytosed ^{125}I-labelled Tf in the iodixanol gradient. To confirm the distribution of endosomes in the iodixanol gradient, we determined the sedimentation characteristics of organelles containing internalized Tf. 3T3-L1 adipocytes were incubated with ^{125}I-labelled Tf for 2 min at 37°C, washed, and allowed to endocytose the ligand for a further 2 to 20 min at 37°C. More than 90% of the internalized tracer accumulated in peak 2 irrespective of the time of uptake (Fig. 4). A similar result was obtained when cells were incubated with ^{125}I-labelled Tf for 60 min at 37°C (data not shown). The distribution of internalized Tf was broader than the distribution of the immunoreactive TfR, and the density of vesicles containing the tracer was slightly greater than that of those previously found to contain immunoreactive TfR (Fig. 3B). Furthermore, the density of the 2-min endosomes was consistently different from that of the 20-min endosomes in that the former coincided more with peak 2a whereas the latter coincided more with peak 2b. Thus, these data suggest that peak 2 comprises different subpopulations of recycling endosomes that may be kinetically segregated and the majority of the TfR is localized to a later endosomal compartment under steady-state conditions. These data are consistent with a very recent report by Sheff et al. (39). Most striking, however, is the observation that very little recycling Tf coincides with peak 1.

Iodixanol equilibrium sedimentation analysis combined with the Tf-HRP-mediated endosomal ablation in 3T3-L1 adipocytes. To confirm that the majority of GLUT4-containing vesicles in peak 2 correspond to endosomes, we performed Tf-HRP endosomal ablation analysis with 3T3-L1 adipocytes. This method exploits the enzymatic activity of HRP to specifically load peroxidase-containing endosomes with DAB polymer (4) and has been utilized with many cell types to label compartments containing the TfR (46–48), the asialoglycoprotein receptor (45, 47), major histocompatibility complex class II (57), and GLUT4 (25). In our initial studies, we tested the effects of different DAB concentrations on the ablation efficiency of different proteins in 3T3-L1 adipocytes. The level of TfR in the LDM fraction was significantly reduced following ablation at a relatively low concentration of DAB (50 μg/ml) and almost completely ablated at a DAB concentration of 250 μg/ml (Fig. 5A, lane 3). However, we did not observe significant ablation of GLUT4, VAMP2, cellubrevin, or syntaxin 6 at lower DAB concentrations (Fig. 5A, lane 3). At higher DAB concentrations we observed significant ablation of each of these proteins (Fig. 5A, lane 4), suggesting that all of these proteins colocalize with recycling transferrin to some extent.

To determine the location of the compartment that is most susceptible to ablation with Tf-HRP, we combined the ablation analysis with iodixanol gradient analysis using the high (250-μg/ml) DAB concentration. For these studies we utilized a

Downloaded from http://mcb.asm.org/ on October 26, 2015 by University of Queensland Library

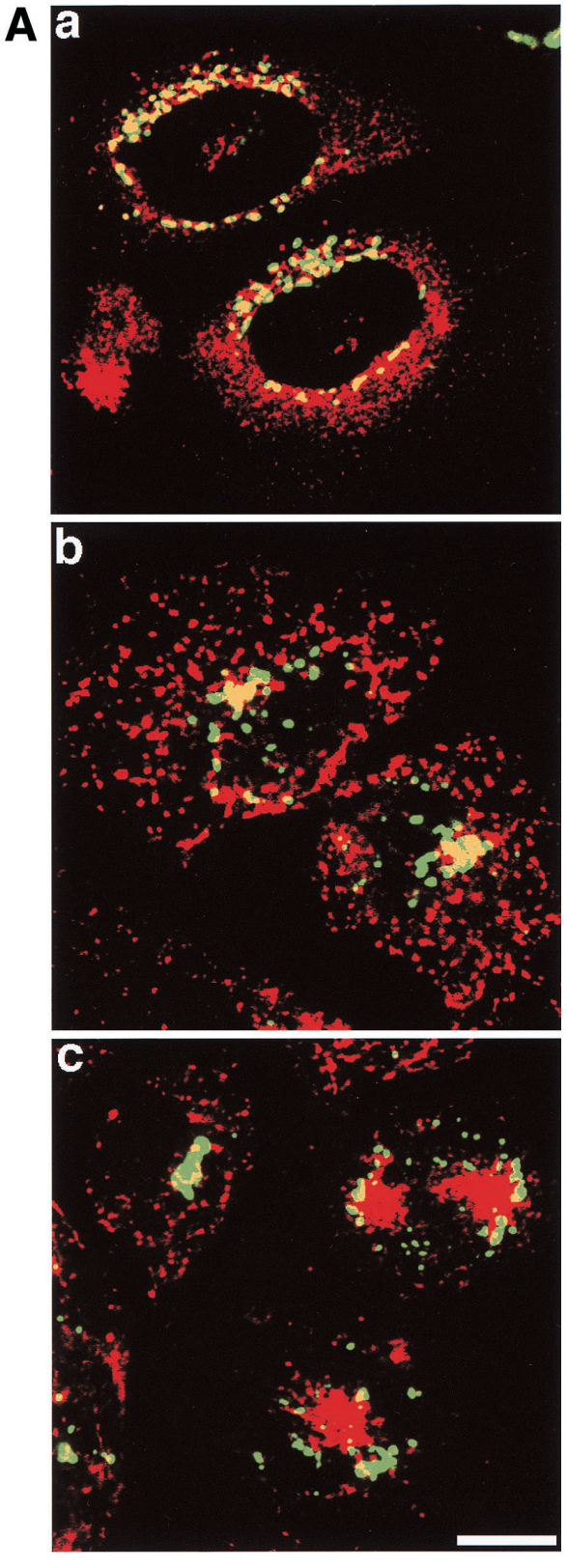

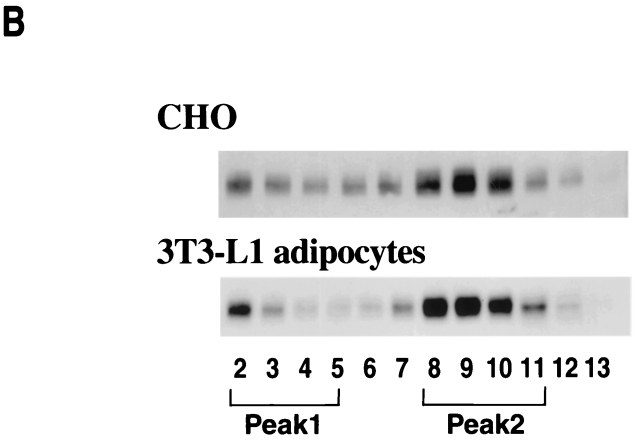

FIG. 6. Distribution of epitope-tagged sialyltransferase in 3T3-L1 adipocytes and CHO cells. (A) CHO cells stably transfected with GLUT4 or with the human TfR were transiently transfected with VSV-G-tagged sialyltransferase cDNA. GLUT4-sialyltransferase-expressing cells were double labelled with antibodies specific for each of these proteins and visualized using Texas red-conjugated anti-rabbit (GLUT4) or FITC-conjugated anti-mouse (sialyltransferase) secondary antibodies (image a), and TfR-sialyltransferase-expressing cells were incubated with Texas red-conjugated Tf for 15 min (image b) or 60 min (image c) and fixed and labelled with anti-VSV-G antibodies, followed by FITC-conjugated anti-mouse antibodies. Confocal images were obtained with a Bio-Rad MRC-600 laser confocal imaging system. Bar = 10 μm. (B) Membranes from either CHO cells or 3T3-L1 adipocytes, expressing VSV-G-tagged sialyltransferase, were analyzed by iodixanol gradient sedimentation. Gradient fractions were immunoblotted with an anti-VSV-G antibody to detect sialyltransferase. Numbers represent different fractions.

slightly longer centrifugation time to form the gradients in order to optimize resolution at the bottom of the gradient. This resulted in a change in the positions of peaks 1 and 2 relative to those shown in Fig. 3. Immunoblotting with antibodies specific for GLUT4, IRAP, syntaxin 6, and cellubrevin revealed that there was a selective loss of immunoreactivity from peak 2 following ablation (Fig. 5B). These data are consistent with the above results (Fig. 3B), suggesting that recycling endosomes are enriched in peak 2 and that most of the GLUT4 found in peak 2 is localized to a recycling endosomal compartment. In contrast, peak 1-enriched proteins were not significantly ablated by treatment with Tf-HRP. It is noteworthy that a small amount of each protein located in peak 2, including GLUT4, remained unaffected following treatment with Tf-HRP and DAB. This may correspond to TGN-derived vesicles which may not be easily accessed by internalized Tf-HRP.

The TGN is enriched in peak 2a. We have suggested from the above studies that in addition to recycling endosomes, peak 2 also contains TGN-derived vesicles. This is based on the distribution of syntaxin 6, CD-MPR, and sortilin. However, each of these proteins may also be localized to endosomes. Thus, to further confirm the distribution of TGN-derived vesicles in the iodixanol gradient we used a marker that is almost exclusively found in the TGN. Sialyltransferase has previously been shown to be confined to the *trans* Golgi region, with very low levels found in endosomes (36, 38). To confirm the TGN localization of sialyltransferase we performed immunofluorescence localization studies with CHO cells. GLUT4 exhibited diffuse perinuclear labelling, in agreement with previous studies (35). In contrast, sialyltransferase was highly concentrated in a rim surrounding the nucleus, consistent with Golgi staining. There was overlap between sialyltransferase and GLUT4 in this region, but there was no diffuse endosomal labelling observed for sialyltransferase. This latter observation was confirmed by comparing the distribution of Tf-containing recycling endosomes with sialyltransferase (Fig. 6A). We also found significant overlap between sialyltransferase and TGN38 in

Downloaded from http://mcb.asm.org/ on October 26, 2015 by University of Queensland Library

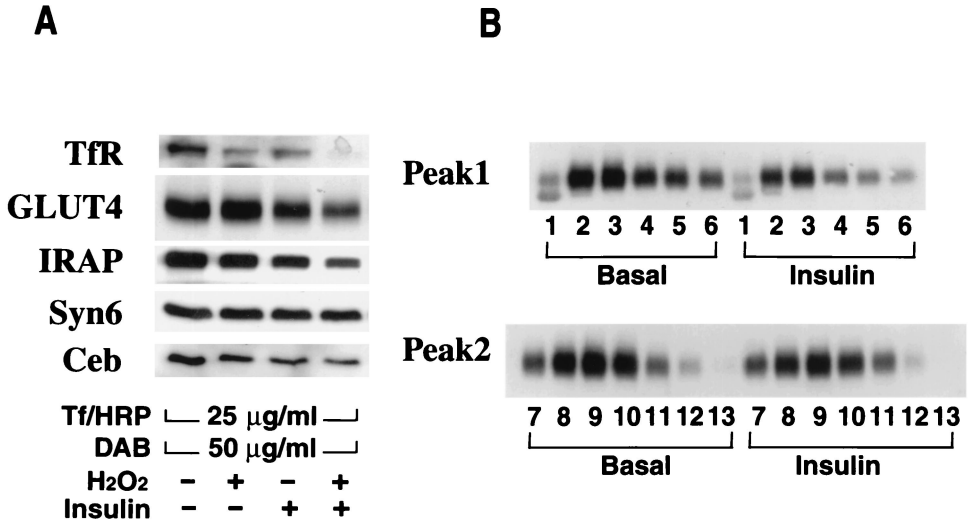

FIG. 7. Effect of insulin on the intracellular distribution of GLUT4 in 3T3-L1 adipocytes. (A) 3T3-L1 adipocytes were serum starved for 16 h in DMEM, incubated with or without 10^{-7} M insulin for 20 min, and then subjected to Tf-HRP ablation as described in the legend for Fig. 5 by using 25 μg of Tf-HRP conjugate per ml and 50 μg of DAB per ml in the presence (+) or absence (−) of 0.02% H_2O_2. The insulin level was maintained throughout the incubation with the Tf-HRP conjugate. The LDM fraction was obtained as described above and analyzed by SDS-PAGE followed by immunoblotting. Syn 6, syntaxin6; Ceb, cellubrevin. (B) 3T3-L1 adipocytes were serum starved for 16 h in DMEM at 37°C and then left untreated or stimulated with 10^{-7} M insulin for 20 min. The LDM fraction was obtained and subjected to iodixanol gradient sedimentation as described. The iodixanol fractions were analyzed as described in the legend to Fig. 3 by SDS-PAGE followed by immunoblotting for GLUT4. The results shown are representative of three separate experiments. Numbers represent different fractions.

CHO cells (data not shown). When the total membrane fraction from these cells was analyzed by iodixanol density gradient sedimentation, immunoreactive VSV-G was enriched in peak 2a (Fig. 6B, upper gel).

We also expressed VSV-G-tagged sialyltransferase in 3T3-L1 adipocytes. When the LDM fraction from these cells was analyzed by iodixanol gradient, results similar to those found for CHO cells were observed (Fig. 6B, lower gel). Sialyltransferase was highly concentrated in peak 2a. This distribution was similar to that of sortilin and also coincided with the peak of CD-MPR and syntaxin 6 (Fig. 3B). These results indicate that TGN-derived vesicles are highly concentrated in peak 2a and show that the density of the TGN is very similar in different cell types.

Peak 1 exhibits higher insulin responsiveness than peak 2. The only protein we have identified to be ablated significantly at low DAB concentrations in basal adipocytes is the TfR. Under these conditions we found no significant ablation of GLUT4, IRAP, syntaxin 6, or cellubrevin (compare Fig. 7A, lanes 1 and 2). When insulin-treated cells were ablated under identical conditions there was a significant increase in ablation efficiency of the TfR, GLUT4, and IRAP, whereas the ablation efficiency of syntaxin 6 was unaffected (Fig. 7A, compare lanes 1 and 2 with lanes 3 and 4). These results suggest that insulin either promotes the accumulation of GLUT4 in endosomes or increases the uptake of the Tf-HRP conjugate.

To confirm the effects of insulin on GLUT4 in peak 1 we compared the iodixanol GLUT4 profiles of membranes harvested from basal cells with those of membranes harvested from insulin-treated cells. As indicated in Fig. 7B, there was quantitatively a greater loss of GLUT4 from peak 1 (mean ± SD, 56.4% ± 2.5%; $n = 3$) than from peak 2 (mean ± SD, 75.0% ± 11.7%; $n = 3$) in response to insulin. It is noteworthy that we have found some variability in the magnitude of the insulin effect in peak 2 (15.4 to 38.0% decrease in response to insulin), thus limiting an exhaustive quantitative analysis of insulin effects on GLUT4 and other proteins using this approach. Regardless, the above results indicate that the magnitude of the insulin responsiveness is greater in peak 1 than in peak 2 in each experiment, and these results collectively indicate that peak 2 represents an endosomal-TGN pool of GLUT4, whereas peak 1 represents a distinct insulin-responsive compartment.

Polypeptide composition of GLUT4-containing vesicles isolated from peak 1 and peak 2. In order to further define these different vesicle subpopulations isolated by iodixanol gradient analysis, we immunoisolated GLUT4-containing vesicles from either peak 1 or peak 2 or the corresponding starting material and subjected them to SDS-PAGE and silver staining (Fig. 8). The last three lanes of Fig. 8 indicate the polypeptide composition of each of the three fractions that were used for immunoadsorption. Overall, the polypeptide composition was quite similar among these fractions, although there were slight differences in the enrichment of different proteins between peak 1 and peak 2. The polypeptide composition of each of three GLUT4-immunoadsorbed fractions, denoted by 1F8, was completely different from that of the respective starting fractions, indicating that membranes separated by iodixanol analysis contain a number of vesicles that presumably do not contain GLUT4. It is also noteworthy that the polypeptide profile of GLUT4 vesicles isolated from 3T3-L1 adipocytes (Fig. 8) is very similar to that of those isolated from rat adipocytes (Fig. 1). A number of proteins were highly enriched in each of the GLUT4 vesicle fractions compared to those in fractions obtained with the irrelevant antibody. The most abundant proteins, which were found in all three fractions, have molecular masses of 50 kDa and 165 kDa, which presumably correspond to GLUT4 and IRAP, respectively. Consistent with the immunoblotting data shown in Fig. 3, the overall protein profiles of vesicles immunopurified from peak 1 and peak 2 were similar. However, IRAP was more enriched in peak 1 compared to peak 2 whereas bands in the 100-kDa range, which presumably correspond to sortilin and amine oxidase, were considerably more enriched in peak 2 than in peak 1. While the GLUT4

Downloaded from http://mcb.asm.org/ on October 26, 2015 by University of Queensland Library

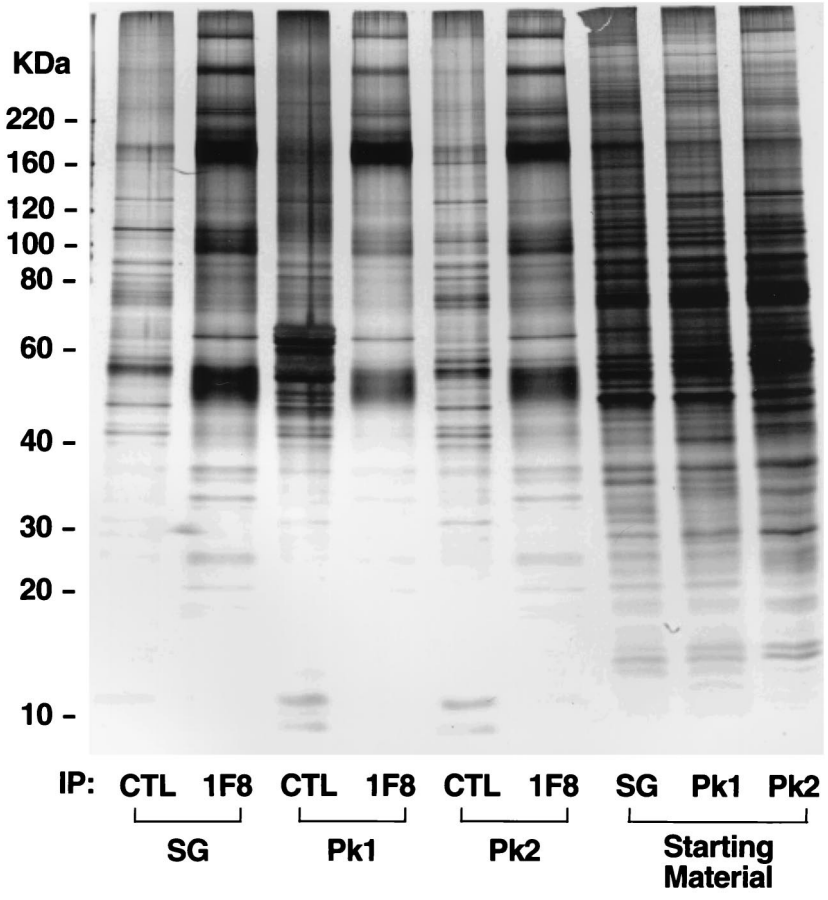

FIG. 8. Polypeptide composition of GLUT4-containing vesicles isolated from peak 1 and peak 2. Intracellular membranes were isolated from 3T3-L1 adipocytes and subjected to either velocity sucrose gradient or iodixanol density gradient sedimentation. Fractions enriched in GLUT4 from either the sucrose gradient (SG) or the iodixanol gradient (peak 1 [Pk1] and peak 2 [Pk2]) were pooled and incubated with a GLUT4-specific antibody (1F8) or an irrelevant antibody (CTL) coupled to cellulose fibers. Immunoadsorbed vesicles were eluted with 0.2 M bicarbonate buffer (pH 11.0) and pelleted, and the eluted proteins or the relevant starting materials were subjected to SDS-PAGE and silver staining. The migration of molecular weight standards is indicated at the left hand side (numbers indicate masses).

band appears to be more enriched in peak 2, this band also contains the CD-MPR (Fig. 1). Other major differences are that bands with molecular masses of 40, 30 to 35, and 25 kDa were highly enriched in peak 2 and almost nondetectable in peak 1. While the identity of these bands is not known, based on previous studies the bands at 30 to 35 kDa likely correspond to secretory carrier membrane proteins. Thus, these studies support the immunoblotting studies (Fig. 3) and suggest that while GLUT4 and IRAP are found in both peak 1 and peak 2, other proteins are differentially distributed between these peaks and this presumably reflects the unique function of these different fractions.

Iodixanol equilibrium gradient sedimentation analysis of rat skeletal muscle and CHO cells overexpressing GLUT4. When the LDM fraction isolated from rat skeletal muscle was subjected to iodixanol density gradient analysis, a distribution of GLUT4, cellubrevin, and syntaxin 6 similar to that observed in 3T3-L1 adipocytes was observed (Fig. 9A). A difference in the distribution of syntaxin 6 (TGN marker, peak 2a) and cellubrevin (recycling endosomal marker, peak 2b) in peak 2 similar to that found in 3T3-L1 adipocytes was also observed in this cell type. In preliminary studies we have been unable to obtain this same type of resolution of different GLUT4 compartments using membranes isolated from primary cultured rat adipocytes. This may reflect a slightly different density of vesicles in these cells. We also performed similar studies with CHO cells stably transfected with the GLUT4 cDNA. In contrast to 3T3-L1 adipocytes or skeletal muscle, a relatively small amount of GLUT4 was found in vesicles corresponding to peak 1 in CHO cells, the majority being found in peak 2 (Fig. 9B). The distribution of syntaxin 6 and cellubrevin in CHO cells was similar to that found in adipocytes and skeletal muscle. Hence, these experiments suggest that while vesicles with the characteristics of the insulin-responsive GLUT4 storage compartment may exist in CHO cells, they are far less numerous than in insulin-sensitive cell types.

DISCUSSION

The insulin-responsive glucose transporter GLUT4 exhibits two features, which may not necessarily be mutually exclusive, that distinguish it from many other recycling proteins. Firstly, in the absence of insulin it is excluded from the PM due to its retention in intracellular tubules and vesicles. Secondly, in response to insulin there is a large increase in PM levels of GLUT4 (>10-fold) compared to a modest two- to threefold increase observed for recycling proteins such as the TfR (51, 52). It has been postulated that both of these features are due to the selective targeting of GLUT4 to a population of vesicles that are withdrawn from the recycling pathways and that are

Downloaded from http://mcb.asm.org/ on October 26, 2015 by University of Queensland Library

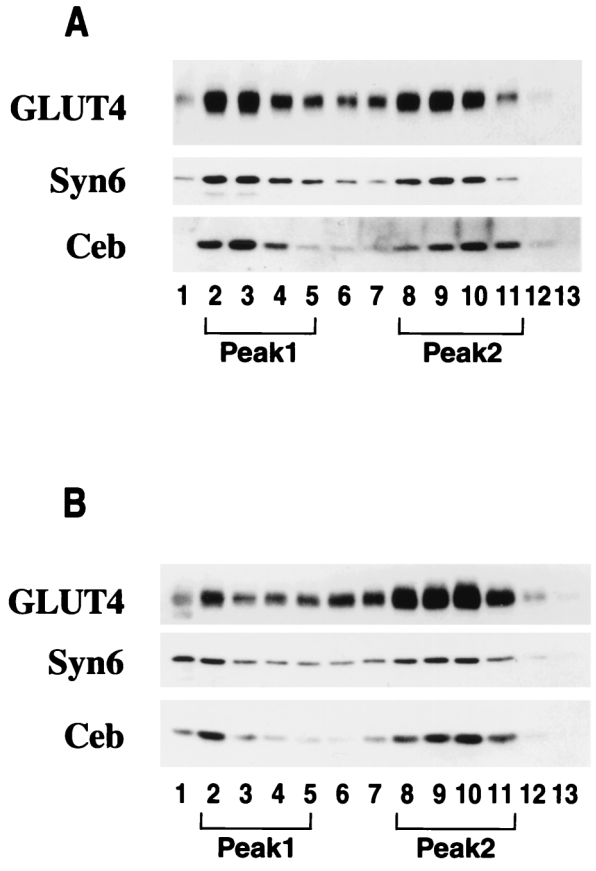

FIG. 9. Intracellular distribution of GLUT4 in other cell types. The LDM fraction from rat skeletal muscle (A) and an intracellular membrane fraction from CHO cells stably overexpressing GLUT4 (B) were obtained by differential centrifugation and subjected to iodixanol equilibrium gradient centrifugation. The iodixanol fractions were analyzed as described for Fig. 3 by SDS-PAGE followed by immunoblotting with antibodies specific for GLUT4, syntaxin 6 (Syn6) or cellubrevin (Ceb).

insulin responsive (42, 58, 59). Despite numerous attempts with a variety of techniques, it has proven difficult to biochemically segregate different populations of GLUT4 vesicles from insulin-sensitive cells; thus, attempts at characterization have been thwarted. As illustrated in Fig. 1, the major proteins found in GLUT4-containing vesicles isolated by immunoadsorption are endosomal or TGN proteins, presumably due to the presence of GLUT4 in these organelles (42).

In the present study we used self-forming iodixanol density gradients to resolve two discrete intracellular GLUT4-containing vesicle peaks. The advantage of this method compared to others, such as the use of sucrose density gradients, is that it is possible to segregate intracellular organelles based on different densities under iso-osmotic conditions (7). The lighter of the two GLUT4-containing vesicle peaks, referred to as peak 2, is a heterogeneous mixture of endosomes and TGN. Within peak 2 we found that TGN proteins such as sortilin, syntaxin 6, and CD-MPR were concentrated in a peak shifted by 1 or 2 fractions from endosomal markers such as Rab4 and cellubrevin. To confirm the distribution of the TGN in these gradients we also examined the distribution of sialyltransferase, a highly specific TGN marker (36). By immunofluorescence microscopy, this protein exhibited a very tight perinuclear distribution (Fig. 6A) consistent with Golgi staining (36). The epitope-tagged sialyltransferase was enriched in peak 2 of the iodixanol gradient overlapping with the peak of syntaxin6. Two separate experiments were performed to confirm the enrichment of endosomes in peak 2. Firstly, we showed that internalized Tf was highly enriched in peak 2 (Fig. 4). It has previously been suggested that Tf may recycle via different classes of endosomes that can be defined kinetically (9). To test the possibility that peak 1 and peak 2 represent different recycling endosomes, we examined the distribution of a rapid (2-min) versus a long (>20-min) pulse of iodinated Tf. Whereas in both cases the internalized Tf was highly enriched in peak 2, we found that the endosomes incubated for 2 min were slightly shifted within peak 2 compared to membranes containing Tf that had been internalized over a longer time course. These data are consistent with a recent study by Sheff et al. (39). Secondly, using Tf-HRP ablation analysis, we observed selective ablation of proteins from peak 2 but not peak 1 (Fig. 5B). A significant proportion of GLUT4 in peak 2 was ablated following uptake of Tf-HRP, consistent with previous studies (25). Collectively, these experiments indicate that the TGN as well as recycling endosomes are highly enriched in peak 2 of the iodixanol gradient, and the localization of GLUT4 to these organelles (42) likely accounts for its presence in this peak.

Several observations suggest that the denser GLUT4-containing vesicle peak (peak 1) resolved by iodixanol density gradient analysis may represent a population of intracellular GLUT4 storage vesicles. Firstly, as described in detail above, this population of vesicles is distinct from either recycling endosomes or the TGN. Secondly, this compartment is more abundant in skeletal muscle and 3T3-L1 adipocytes (Fig. 3A and 8A) compared to CHO cells (Fig. 8B), indicating that its formation may underpin the unique features of GLUT4 that are predominantly evident only when this protein is expressed in insulin-sensitive cells. Thirdly, in response to insulin there is a more significant decline in the levels of GLUT4 in peak 1 versus peak 2, indicating that this population of vesicles may be highly insulin responsive. However, it is noteworthy that this latter conclusion is based on steady-state measurements and it is conceivable that insulin stimulates the entry of GLUT4 into peak 2 from peak 1, either directly or indirectly, thus resulting in an underestimation of the potential insulin responsiveness of peak 2. In fact, consistent with the latter observation, it has been previously reported that the presence of GLUT4 in endosomes is increased by insulin (42). This is also supported by our observations that the efficiency of GLUT4 ablation with Tf-HRP is increased by insulin (Fig. 8A). Regardless, it is evident that peak 1 represents a compartment that serves to withdraw GLUT4 from the constitutive recycling pathway in the absence of insulin and that it is highly insulin responsive.

How is this separate GLUT4 storage compartment formed? Many of the proteins enriched in peak 2 are also located in peak 1 (Fig. 3 and 8). In fact, although internalized Tf recycles predominantly via peak 2 (Fig. 4), there is some TfR in peak 1 (Fig. 3B). Hence, this supports the conclusion that peak 1 vesicles are probably derived from recycling endosomes and/or the TGN. In support of this, Herman and colleagues, using an epitope-tagged GLUT4 construct expressed in CHO cells, recently unveiled a temperature-sensitive endosomal sorting step that selectively regulates the trafficking of GLUT4 but not Tf (11, 56). Using glycerol gradient sedimentation, they identified a population of small GLUT4-containing vesicles, possibly analogous to our peak 1 vesicles, and the entry of GLUT4 into these vesicles is blocked at the low temperature. Thus, it is conceivable that GLUT4 is continuously cycling between peak 1 and endosomes in the absence of insulin, and the recycling step may be blocked at low temperatures, thus trapping GLUT4 in a non-insulin-responsive compartment. Consistent

Downloaded from http://mcb.asm.org/ on October 26, 2015 by University of Queensland Library

with this idea, researchers in our laboratory have shown that incubation of 3T3-L1 adipocytes at 19°C for 2 h results in a complete block of insulin-stimulated GLUT4 translocation. In preliminary experiments, we have found that the clear resolution of two GLUT4-containing vesicle peaks is lost following incubation of adipocytes at 20°C for 2 h (M. Hashiramoto and D. E. James, unpublished data).

In conclusion, our observations strongly suggest that, in insulin-sensitive cells, there may be a unique GLUT4-containing vesicular population comprising peak 1 in the iodixanol gradient. They appear to be a derivative of the endosomes but demonstrate a different sedimentation property from those derived from the TfR-containing recycling endosomes or the TGN. Our results also suggest that the ability of GLUT4 to be sorted into this unique subcellular compartment would be prerequisite to the major function of GLUT4, namely, higher insulin responsiveness than is exhibited by the proteins now segregated mostly into peak 2. This one-step purification method of the unique intracellular GLUT4 compartment may prove useful in further defining the nature of intracellular GLUT4 compartments and in characterizing the trafficking pathway involved in the insulin-stimulated translocation of GLUT4.

ACKNOWLEDGMENTS

We are grateful to G. Lienhard, A. Hille-Rehfeld, M. Takahashi, P. Van der Sluijs, T. Nilsson, and T. McGraw for providing antibodies and cDNAs used in this study. We are indebted to Teresa Munchow for excellent assistance in tissue culture and Timo Meerloo and Annette M. Shewan for assistance in sialyltransferase experiments. We very much appreciate Shane Rea, Sharon Clark, and Laura B. Martin for help and Robert G. Parton for critical reading of the manuscript. Finally, we cordially thank Miyako Kishimoto-Hashiramoto for support throughout the study.

This work was supported by grants from the Juvenile Diabetes Foundation International postdoctoral fellowship (to M.H.) and the National Health and Medical Research Council of Australia (to D.E.J.).

REFERENCES

1. **Birnbaum, M. J., and D. E. James.** 1995. The insulin-regulatable glucose transporter GLUT-4. Curr. Opin. Endocrinol. Diabetes **2:**383–391.
2. **Bock, J. B., J. Klumperman, S. Davanger, and R. H. Scheller.** 1997. Syntaxin 6 functions in trans-Golgi network vesicle trafficking. Mol. Biol. Cell **8:**1261–1271.
3. **Clark, S. F., S. Martin, A. J. Carozzi, M. M. Hill, and D. E. James.** 1998. Intracellular localization of phosphatidylinositide 3-kinase and insulin receptor substrate-1 in adipocytes: potential involvement of a membrane skeleton. J. Cell Biol. **140:**1211–1225.
4. **Courtoy, P. J., J. Quintart, and P. Baudhuin.** 1984. Shift of equilibrium density induced 3,3′-diaminobenzidine cytochemistry: a new procedure for the analysis and purification of peroxidase-containing organelles. J. Cell Biol. **98:**870–876.
5. **Cushman, S. W., and L. J. Wardzala.** 1980. Potential mechanism of insulin action on glucose transport in the isolated rat adipose cell: apparent translocation of intracellular transport systems to the plasma membrane. J. Biol. Chem. **255:**4758–4762.
6. **Del Vecchio, R. L., and P. F. Pilch.** 1991. Phosphatidylinositol 4-kinase is a component of glucose transporter (GLUT4)-containing vesicles. J. Biol. Chem. **266:**13278–13283.
7. **Ford, T., J. Graham, and D. Rickwood.** 1994. Iodixanol: a nonionic isoosmotic centrifugation medium for the formation of self-generated gradients. Anal. Biochem. **220:**360–366.
8. **Frost, S. C., and M. D. Lane.** 1985. Evidence for the involvement of viscinal sulfhydryl groups in insulin-activated hexose transport in 3T3-L1 adipocytes. J. Biol. Chem. **260:**2646–2652.
9. **Gruenberg, J., and F. R. Maxfield.** 1995. Membrane transport in the endocytic pathway. Curr. Opin. Cell Biol. **7:**552–563.
10. **Hanpeter, D., and D. E. James.** 1995. Characterisation of the intracellular GLUT-4 compartment. Mol. Membr. Biol. **12:**263–269.
11. **Herman, G. A., F. Bonzelius, A. M. Cieutat, and R. B. Kelly.** 1994. A distinct class of storage vesicles, identified by expression of the glucose transporter GLUT4. Proc. Natl. Acad. Sci. USA **91:**12750–12754.
12. **Hill, M. M., S. F. Clark, and D. E. James.** 1997. Insulin-regulatable phosphoproteins in 3T3-L1 adipocytes from detergent-insoluble complexes not associated with caveolin. Electrophoresis **18:**2629–2637.
13. **Hudson, A. W., D. C. Fingar, G. A. Seidner, G. Griffiths, B. Burke, and M. J. Birnbaum.** 1993. Targeting of the insulin-responsive glucose transporter (GLUT4) to the regulated secretory pathway in PC12 cells. J. Cell Biol. **122:**579–588.
14. **James, D. E., R. Brown, J. Navarro, and P. F. Pilch.** 1988. Insulin-regulatable tissues express a unique insulin-sensitive glucose transport protein. Nature **333:**183–185.
15. **James, D. E., and P. F. Pilch.** 1988. Fractionation of endocytic vesicles and glucose-transporter-containing vesicles in rat adipocytes. Biochem. J. **256:**725–732.
16. **James, D. E., M. Strube, and M. Mueckler.** 1989. Molecular cloning and characterisation of an insulin-regulatable glucose transporter. Nature **338:**83–87.
17. **James, D. E., R. C. Piper, and J. W. Slot.** 1994. Insulin stimulation of GLUT-4 translocation: a model for regulated recycling. Trends Cell Biol. **4:**120–126.
18. **Kandror, K. V., and P. F. Pilch.** 1994. Identification and isolation of glycoproteins that translocate to the cell surface from GLUT4-enriched vesicles in an insulin-dependent fashion. J. Biol. Chem. **269:**138–142.
19. **Kandror, K. V., and P. F. Pilch.** 1994. gp160, a tissue-specific marker for insulin-activated glucose transport. Proc. Natl. Acad. Sci. USA **91:**8017–8021.
20. **Kandror, K. V., and P. F. Pilch.** 1996. Compartmentalization of protein traffic in insulin-sensitive cells. Am. J. Physiol. **271:**E1–E14.
21. **Keller, S. R., H. M. Scott, C. C. Mastick, R. Aebersold, and G. E. Lienhard.** 1995. Cloning and characterisation of a novel insulin-regulated membrane aminopeptidase from Glut4 vesicles. J. Biol. Chem. **270:**23612–23618.
22. **Kristiansen, S., T. Ramlal, and A. Klip.** 1998. Phosphatidylinositol 4-kinase, but not phosphatidylinositol 3-kinase, is present in GLUT4-containing vesicles from rat skeletal muscle. Biochem. J. **335:**351–356.
23. **Laemmli, U. K.** 1970. Cleavage of structural proteins during the assembly of the head of bacteriophage T4. Nature **227:**680–685.
24. **Lin, B.-Z., P. F. Pilch, and K. V. Kandror.** 1997. Sortilin is a major protein component of Glut4-containing vesicles. J. Biol. Chem. **272:**24145–24247.
25. **Livingstone, C., D. E. James, J. E. Rice, D. Hanpeter, and G. W. Gould.** 1996. Compartment ablation analysis of the insulin-responsive glucose transporter (GLUT4) in 3T3-L1 adipocytes. Biochem. J. **315:**487–495.
26. **Martin, S., J. Tellam, C. Livingstone, J. W. Slot, G. W. Gould, and D. E. James.** 1996. Glucose transporter-4 and vesicle-associated membrane protein-2 are segregated from recycling endosomes in insulin-regulatable cells. J. Cell Biol. **134:**625–635.
27. **Martin, S., J. E. Rice, G. W. Gould, J. W. Slot, and D. E. James.** 1997. The glucose transporter GLUT4 and the aminopeptidase vp165 colocalise in tubulovesicular elements in adipocytes and cardiomyocytes. J. Cell Sci. **110:**2281–2291.
28. **Mastick, C. C., R. Aebersold, and G. E. Lienhard.** 1994. Characterisation of a major protein in GLUT4 vesicles. J. Biol. Chem. **269:**6089–6092.
29. **Morgenstern, J. P., and H. Land.** 1990. Advanced mammalian gene transfer: high titre retroviral vectors with multiple drug selection markers and a complementary helper-free packaging cell lines. Nucleic Acids Res. **18:**3587–3596.
30. **Morris, N. J., A. Ducret, R. Aebersold, S. A. Ross, S. R. Keller, and G. E. Lienhard.** 1997. Membrane amine oxidase cloning and identification as a major protein in the adipocyte plasma membrane. J. Biol. Chem. **272:**9388–9392.
31. **Morris, N. J., S. A. Ross, W. S. Lane, S. K. Moestrup, C. M. Petersen, S. R. Keller, and G. E. Lienhard.** 1998. Sortilin is the major 110-kDa protein in GLUT4 vesicles from adipocytes. J. Biol. Chem. **273:**3582–3587.
32. **Oho, C., S. Seino, and M. Takahashi.** 1995. Expression and complex formation of soluble N-ethyl-maleimide-sensitive factor attachment protein (SNAP) receptors in clonal rat endocrine cells. Neurosci. Lett. **186:**208–210.
33. **Pear, W. S., G. P. Nolan, M. L. Scott, and D. Baltimore.** 1993. Production of high-titer helper-free retroviruses by transient transfection. Proc. Natl. Acad. Sci. USA **90:**8392–8396.
34. **Piper, R. C., L. J. Hess, and D. E. James.** 1991. Differential sorting of two glucose transporters expressed in insulin-sensitive cells. Am. J. Physiol. **260:**C570–C580.
35. **Piper, R. C., C. Tai, P. Kulesza, S. Pang, D. Warnock, J. Baenziger, J. W. Slot, H. J. Geuze, C. Puri, and D. E. James.** 1993. GLUT-4 NH2 terminus contains a phenylalanine-based targeting motif that regulates intracellular sequestration. J. Cell Biol. **121:**1221–1232.
36. **Rabouille, C., N. Hui, F. Hunte, R. Kieckbusch, E. G. Berger, G. Warren, and T. Nilsson.** 1995. Mapping the distribution of Golgi enzymes involved in the construction of complex oligosaccharides. J. Cell Sci. **108:**1617–1627.
37. **Ross, S. A., H. M. Scott, M. J. Morris, W.-Y. Leung, F. Mao, G. E. Lienhard, and S. R. Keller.** 1996. Characterisation of the insulin-regulated membrane aminopeptidase in 3T3-L1 adipocytes. J. Biol. Chem. **27:**3328–3332.
38. **Roth, J., D. J. Taatjes, J. M. Lucocq, J. Weinstein, and J. C. Paulson.** 1985. Demonstration of an extensive trans-tubular network continuous with the

Downloaded from http://mcb.asm.org/ on October 26, 2015 by University of Queensland Library

Golgi apparatus stack that may function in glycosylation. Cell **43:**287–295.
39. **Sheff, D. R., E. A. Daro, M. Hull, and I. Mellman.** 1999. The receptor recycling pathway contains two distinct populations of early endosomes with different sorting functions. J. Cell Biol. **145:**123–139.
40. **Simpson, I. A., D. R. Yver, P. J. Hissin, L. J. Wardzala, E. Karnieli, L. B. Salans, and S. W. Cushman.** 1983. Insulin-stimulated translocation of glucose transporters in isolated rat adipose cells: characterisation of subcellular fractions. Biochim. Biophys. Acta **763:**393–407.
41. **Sleeman, M. W., N. P. Donegen, R. Heller-Harrison, W. S. Lane, and M. P. Czech.** 1998. Association of acyl-CoA synthetase-1 with GLUT4-containing vesicles. J. Biol. Chem. **273:**3132–3135.
42. **Slot, J. W., H. J. Geuze, S. Gigengack, G. E. Lienhard, and D. E. James.** 1991. Immuno-localisation of the insulin regulatable glucose transporter in brown adipose tissue of the rat. J. Cell. Biol. **113:**123–135.
43. **Slot, J. W., H. J. Geuze, S. Gigengack, D. E. James, and G. E. Lienhard.** 1991. Translocation of the glucose transporter GLUT4 in cardiac myocytes of the rat. Proc. Natl. Acad. Sci. USA **88:**7815–7819.
44. **Slot, J. W., G. Garruti, S. Martin, V. Oorschot, G. Posthuma, E. W. Kraegan, R. Laybutt, G. Thibault, and D. E. James.** 1997. GLUT-4 is targeted to secretory granules in rat atrial cardiomyocytes. J. Cell Biol. **137:**1–12.
45. **Stoorvogel, W., H. J. Geuze, and G. J. Strous.** 1987. Sorting of endocytosed transferrin and asialoglycoprotein occurs immediately after internalization in HepG2 cells. J. Cell Biol. **104:**1261–1268.
46. **Stoorvogel, W., H. J. Geuze, J. M. Griffith, and G. J. Strous.** 1988. The pathways of endocytosed transferrin and secretory proteins are connected in the trans-Golgi reticulum. J. Cell Biol. **106:**1821–1829.
47. **Stoorvogel, W., G. J. Strous, H. J. Geuze, V. Oorschot, and A. L. Schwartz.** 1991. Late endosomes derived from early endosomes by maturation. Cell **65:**417–427.
48. **Stoorvogel, W., V. Oorschot, and H. J. Geuze.** 1996. A novel class of clathrin-coated vesicles budding from endosomes. J. Cell Biol. **132:**21–33.
49. **Suzuki, K., and T. Kono.** 1980. Evidence that insulin causes the translocation of glucose transport activity to the plasma membrane from an intracellular storage site. Proc. Natl. Acad. Sci. USA **77:**2542–2545.
50. **Szebenyi, G., and P. Rotwein.** 1991. Differential regulation of mannose 6-phosphate receptors and ligands during the myogenic development of C2 cells. J. Biol. Chem. **266:**5534–5539.
51. **Tanner, L. I., and G. E. Lienhard.** 1987. Insulin elicits a redistribution of transferrin receptors in 3T3-L1 adipocytes through an increase in the rate constant for receptor externalisation. J. Biol. Chem. **262:**8975–8980.
52. **Tanner, L. I., and G. E. Lienhard.** 1987. Localization of transferrin receptors and insulin-like growth factor II receptors in vesicles from 3T3-L1 adipocytes that contain intracellular glucose transporters. J. Cell Biol. **108:**1537–1545.
53. **Tellam, J. T., S. L. Macaulay, S. McIntosh, D. R. Hewish, C. W. Ward, and D. E. James.** 1997. Characterization of munc-18c and syntaxin-4 in 3T3-L1 adipocytes. Putative role in insulin-dependent movement of GLUT4. J. Biol. Chem. **272:**6179–6186.
54. **Ullrich, O., S. Reinsch, S. Urbé, M. Zerial, and R. G. Parton.** 1996. Rab11 regulates recycling through the pericentriolar recycling endosome. J. Cell Biol. **135:**914–924.
55. **Van der Sluijs, P., M. Hull, A. Zahraoui, A. Tavitian, B. Goud, and I. Mellman.** 1991. The small GTP-binding protein rab4 is associated with early endosomes. Proc. Natl. Acad. Sci. USA **88:**6313–6317.
56. **Wei, M. L., F. Bonzelius, R. M. Scully, R. B. Kelly, and G. A. Herman.** 1998. GLUT4 and transferrin receptor are differentially sorted along the endocytic pathway in CHO cells. J. Cell Biol. **140:**565–575.
57. **West, M. A., J. M. Lucocq, and C. Watts.** 1994. Antigen processing and class II MHC peptide-loading compartments in human B-lymphoblastoid cells. Nature **369:**147–151.
58. **Yang, J., and G. D. Holman.** 1993. Comparison of GLUT4 and GLUT1 subcellular trafficking in basal and insulin stimulated 3T3-L1 cells. J. Biol. Chem. **268:**4600–4603.
59. **Yeh, J.-I., K. J. Verhey, and M. J. Birnbaum.** 1995. Kinetic analysis of glucose transporter trafficking in fibroblasts and adipocytes. Biochemistry **34:**15523–15531.

Downloaded from http://mcb.asm.org/ on October 26, 2015 by University of Queensland Library